PVT Properties of Dinitrogen Monoxide

Giovanni Di Nicola,*,† Giuliano Giuliani,† Renato Ricci,† and Roman Stryjek‡

Dipartimento di Energetica, Università Politecnica delle Marche, 60100 Ancona, Italy, and Institute of Physical Chemistry, Polish Academy of Sciences, 01-224 Warsaw, Poland

The *PVT* properties of dinitrogen monoxide (N_2O) have been measured. In particular, experiments were performed by means of two different apparatus, both in the two-phase region and in the superheated vapor-phase region: the isochoric method was applied in the saturation region, and the Burnett method was applied in the vapor region. Isochoric measurements were carried out at temperatures from (219 to 273) K and at pressures from (550 to 3100) kPa. The 18 measurements along the saturated liquid−vapor region were fit, together with selected literature data, with the Wagner equation. For Burnett measurements, 14 runs along 7 isotherms in a pressure range from (170 to 5200) kPa were made. The second and third virial coefficients were derived, and good consistency was found after comparison with data in the literature.

Introduction

Dinitrogen monoxide is an inexpensive and widely available gas. It is largely used as a weak anaesthetic gas for surgical purposes. It is also used in the dairy industry as a mixing and foaming agent because it is nonflammable bacteriostatic (stops bacteria from growing) and leaves no taste or odor. It is also used in auto racing to produce faster acceleration and in diving to prepare divers for nitrous-like effects. Dinitrogen monoxide is considered to be one of the main contributors to the greenhouse effect because of its expendable uses. When it is considered to be a working fluid for refrigeration, its GWP = 310 for 100 years can be considered to be low if compared with that of HFCs. It is also a "natural refrigerant" under all respects. ASHRAE, in its more recent version of Standard 34,[1] designates it as R744a.

Despite this consideration, a majority of the thermophysical property measurements available in the literature are rather aged. In this work, a careful revision of the literature sources was carried out, and finally, the present vapor pressure and *PVT* measurements were compared with existing measurements.

Experimental Section

Reagents. N_2O was supplied by Sol SpA, and its purity was checked by gas chromatographic analysis using a thermal conductivity detector. It was found to be 99.99% on an area-response basis.

Apparatuses. In this paper, the adopted apparatuses are not presented because they are the same as those described elsewhere[2,3] with no modifications. Here, only a brief description is reported.

A constant-volume apparatus with a volume of 273.5 cm^3 was used for the two-phase measurements. A stainless steel spherical cell contains the refrigerant sample and is connected to a differential-diaphragm pressure transducer coupled to an electronic null indicator. The spherical cell and pressure transducer are immersed in two thermostatic baths containing different silicon oils and are alternatively used for measurements in different temperature ranges. Both baths are controlled by a proportional integrative derivative (PID) device. An auxiliary bath, also controlled by a PID device, helps the system to keep the temperature constant. A platinum resistance thermometer is immersed near the cell and is connected to a digital indicator.

The Burnett apparatus used for the vapor-phase measurements consists of two pressure vessels—the measurement chamber and the expansion chamber—both spherical in shape with volumes of approximately 70 cm^3 and 35 cm^3, respectively. Some auxiliary systems for filling and mixing the compounds in the Burnett vessels and for controlling and measuring the pressure and temperature complete the setup. Also for the Burnett apparatus, the measurement vessel is connected to a diaphragm-type differential pressure transducer coupled to an electronic null indicator. The pressure on either side of the diaphragm is balanced with nitrogen by means of a precision pressure controller, and the pressure is read by a digital pressure gauge. The vessels with the magnetic pump and the pressure transducer are immersed in a thermostatic bath filled with about 45 L of silicon oil. Again, the temperature of the bath is kept constant by means of a PID device. The temperature control and acquisition system relies on two platinum resistance thermometers. The Burnett constant, N, defined as the ratio of the volumes of cell A and the sum of the volumes of cells A and B at zero pressure, was determined using gaseous helium measurements. After taking measurements at several isotherms, the constant was found to be $N = 1.4969 \pm 0.0001$ for all series excluding the last two series that were performed with $N = 1.4961 \pm 0.0001$ after small modifications of valve volumes.

Experimental Uncertainties

The uncertainty in the temperature measurements is due to the thermometer and any instability of the bath. The stability of the bath was found to be less than ±0.015 K, and the uncertainty of the thermometer was found to be less than ±0.010 K in our temperature range. The total

* Corresponding author. Tel: +39-0712204277. Fax: +39-0712804239. E-mail: anfreddo@univpm.it.
† Università Politecnica delle Marche.
‡ Polish Academy of Sciences.

10.1021/je049842u CCC: $27.50
Published on Web 07/30/2004

Table 1. Experimental Saturation Pressures for N_2O

T_{90}/K	P/kPa	T_{90}/K	P/kPa
219.24	554.7	247.65	1521.9
222.28	626.3	252.73	1777.0
223.31	652.8	257.80	2061.8
227.32	759.6	257.87	2065.4
227.36	760.6	262.90	2379.0
232.37	912.1	262.95	2381.8
232.43	915.4	267.98	2730.6
237.49	1092.9	268.03	2734.0
242.57	1294.7	273.08	3119.9

Table 2. Critical Parameters from Various Literature Sources

T_c/K	P_c/kPa	ref
309.5305	7206.234	5
309.5305	7234.605	6
309.5645	7254.465	7
309.5506	7238.000	10
309.5394		15
309.6406[a]	7270.000	16

[a] Datum not considered for the final average calculation.

uncertainty in the temperature measurements was thus less than ±0.03 K for both apparatuses. Any uncertainty in the pressure measurements is due to the transducer and null indicator system and the pressure gauge. The digital pressure indicator (Ruska, model 7000) has an uncertainty of ±0.003% of the full scale. The total uncertainty in the pressure measurement, also influenced by temperature fluctuations due to bath instability, was found to be less than ±1 kPa for both apparatuses.

For the isochoric method, the uncertainty in the measurement of the mass inside the cell was estimated to amount to ±10 mg. The volume of the cell, piping, and pressure transducer cavity was measured with an uncertainty of ±0.0003 dm^3. From the uncertainties in the mass and volume measurements, the uncertainty in the calculated molar volume was estimated to be always less than ±0.08 $dm^3 \cdot mol^{-1}$. The overall experimental uncertainty in terms of pressure, calculated using the laws of error propagation, was estimated to be lower than ±0.8 kPa for measurements along the saturation line.

For the Burnett method, the uncertainty of the mixture's composition was found to be constantly lower than 0.5% mole fraction. The experimental uncertainties in the second and third virial coefficients are estimated to be within ±1.5 $cm^3 \cdot mol^{-1}$ and ±500 $cm^6 \cdot mol^{-2}$, respectively.

Results for the Saturation Region

In the two-phase region, 18 data points at temperatures from (219 to 273) K and pressures from (550 to 3100) kPa measured by the isochoric apparatus are reported in Table 1.

The analysis of the literature showed that a total of 11 data sources are available.[4−14] Taking into account all of the data with the present data, a total of 146 points were regressed as a combined set with the Antoine equation. From a first analysis of the results, it was possible to detect a few series of rather old sources[11−14] that clearly showed data out of the common trend. These data were not considered in the further evaluation. Finally, 119 data were regressed with the Wagner equation in the following form:

$$\ln\frac{P}{P_c} = \frac{T_c}{T}[A_1\tau + A_2\tau^{1.5} + A_3\tau^{2.5}] \qquad (1)$$

where $\tau = (T_c - T)/T_c$; the critical temperature $T_c = 309.54$ K and the critical pressure $P_c = 7249.27$ kPa were taken as fixed values. The critical values were estimated by averaging the values reported in reliable literature sources, where critical temperatures[5−7,10,15] and critical pressures[6,7,10,16] were measured (Table 2). The following values were found for the parameters: $A_1 = -6.88269266$, $A_2 = 1.94458967$, and $A_3 = -2.58663757$ with bias(dP/P) and absolute(dP/P) deviations equal to −0.03% and 0.14%, as defined in eqs 2 and 3, respectively:

$$\text{bias(d}P\text{)} = \frac{1}{n}\sum_{i=1}^{n}\left[\frac{P_{\text{exptl}} - P_{\text{calcd}}}{P_{\text{exptl}}}\right]100 \qquad (2)$$

$$\text{abs(d}P\text{)} = \frac{1}{n}\sum_{i=1}^{n}\left[\frac{|P_{\text{exptl}} - P_{\text{calcd}}|}{P_{\text{exptl}}}\right]100 \qquad (3)$$

where n is the number of experimental points. Scatter diagrams of absolute and relative deviations in pressure are shown in Figures 1 and 2, respectively, for each considered point.

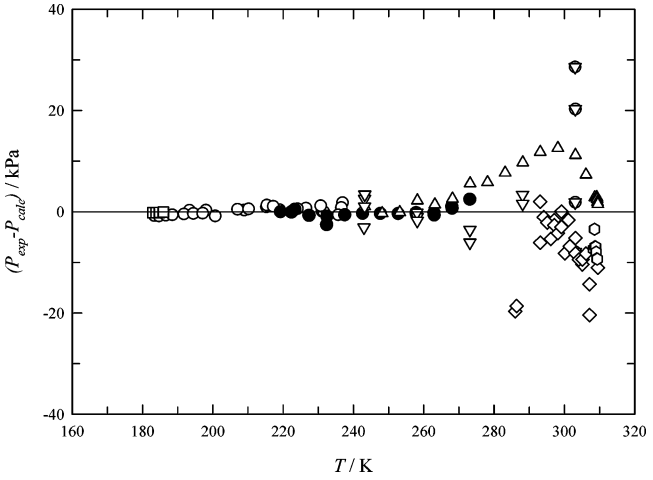

Figure 1. Scatter diagram of the absolute saturated pressure deviations from the fit with the Wagner equation (eq 1): ○, Hoge; △, Couch et al.; ⬡, Ohgaki et al.; □, Blue et Giaque; ▽, Hirth; ◇, Cook; ●, present work.

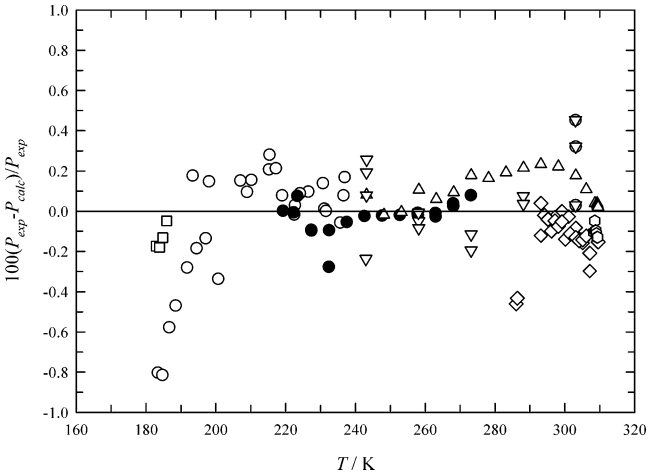

Figure 2. Scatter diagram of the relative saturated pressure deviations (%) from the fit with the Wagner equation (eq 1): ○, Hoge; △, Couch et al.; ⬡, Ohgaki et al.; □, Blue et Giaque; ▽, Hirth; ◇, Cook; ●, present work.

Results for the Superheated Vapor Region

For N_2O, 126 experimental points along 7 isotherms (14 sets in all) were collected in the temperature range from

Table 3. Experimental Pressures Measured during Burnett Expansions for N_2O[a]

series 1		series 2		series 3		series 4		series 5	
P/kPa	*z*	*P*/kPa	*z*	*P*/kPa	*z*	*P*/kPa	*z*	*P*/kPa	*z*
T = 283.51 K		*T* = 283.50 K		*T* = 304.09 K		*T* = 304.10 K		*T* = 314.42 K	
3232.1	0.7451	3680.3	0.6958	3812.3	0.7720	3945.6	0.7604	4027.4	0.7881
2390.6	0.8250	2788.1	0.7891	2781.3	0.8430	2893.4	0.8347	2915.1	0.8539
1705.3	0.8809	2020.0	0.8558	1968.7	0.8932	2054.5	0.8871	2052.9	0.9001
1188.9	0.9193	1422.1	0.9019	1366.6	0.9281	1428.5	0.9233	1420.6	0.9324
816.9	0.9456	983.6	0.9337	935.6	0.9511	980.2	0.9484	971.5	0.9545
556.2	0.9636	672.4	0.9554	635.2	0.9666	666.7	0.9655	659.3	0.9696
376.3	0.9761	456.3	0.9705	429.3	0.9779	450.8	0.9772	445.1	0.9798
253.7	0.9848	308.1	0.9809	288.7	0.9846	303.6	0.9853	299.5	0.9869
170.6	0.9917	207.4	0.9884	194.0	0.9900	204.0	0.9912	201.1	0.9920

series 6		series 7		series 8		series 9		series 10	
P/kPa	*z*	*P*/kPa	*z*	*P*/kPa	*z*	*P*/kPa	*z*	*P*/kPa	*z*
T = 314.41 K		*T* = 324.78 K		*T* = 324.79 K		*T* = 335.18 K		*T* = 335.16 K	
3911.4	0.7949	3833.8	0.8251	3845.5	0.8240	4008.4	0.8389	3777.8	0.8498
2822.9	0.8587	2731.6	0.8800	2740.0	0.8789	2839.6	0.8895	2665.8	0.8977
1984.4	0.9036	1904.7	0.9185	1910.8	0.9174	1972.3	0.9248	1845.9	0.9304
1371.3	0.9347	1309.1	0.9449	1313.6	0.9441	1352.3	0.9492	1263.2	0.9531
936.8	0.9558	891.4	0.9631	894.5	0.9623	919.2	0.9658	857.6	0.9686
635.5	0.9706	602.6	0.9746	605.3	0.9748	621.3	0.9772	579.2	0.9792
429.0	0.9808	406.1	0.9831	407.9	0.9833	418.3	0.9847	389.8	0.9864
288.6	0.9878	272.8	0.9888	274.1	0.9891	281.0	0.9902	261.7	0.9913
193.8	0.9927	182.9	0.9923	183.9	0.9933	188.5	0.9942	175.4	0.9949

series 11		series 12		series 13		series 14	
P/kPa	*z*	*P*/kPa	*z*	*P*/kPa	*z*	*P*/kPa	*z*
T = 345.58 K		*T* = 345.51 K		*T* = 364.36 K		*T* = 364.36 K	
4008.9	0.8565	4029.0	0.8553	5179.9	0.8475	4555.0	0.8679
2819.4	0.9017	2834.5	0.9008	3655.3	0.8947	3191.1	0.9097
1949.3	0.9332	1960.2	0.9324	2535.6	0.9285	2201.5	0.9389
1332.3	0.9548	1340.3	0.9543	1737.0	0.9517	1502.7	0.9588
903.9	0.9697	909.5	0.9693	1179.8	0.9670	1018.5	0.9723
610.1	0.9797	613.8	0.9794	797.5	0.9779	687.1	0.9812
410.4	0.9865	413.0	0.9863	536.5	0.9843	462.0	0.9871
275.5	0.9911	277.2	0.9910	360.3	0.9889	309.9	0.9907
184.6	0.9943	185.8	0.9943	241.7	0.9925	207.6	0.9928

[a] Series 1−12 were obtained with $N = 1.4969$, and series 13 and 14 were obtained with $N = 1.4961$. *z* denotes the compressibility coefficient.

Table 4. Second and Third Virial Coefficients for N_2O with $\rho(1)$ Denoting the Regressed Initial Density

series	*T*/K	*B*/cm³·mol⁻¹	10^3C/cm⁶·mol⁻²	$10^3\rho(1)$/mol·cm⁻³	$100(P - P_{calcd})P^{-1}$	Abs$\{100(P - P_{calcd})P^{-1}\}$
1	283.51	−150.3	6.41	1.84017	0.04	0.05
2	283.50	−151.1	6.91	2.24384	0.03	0.04
3	304.09	−127.3	5.38	1.95324	0.02	0.03
4	304.10	−128.4	5.67	2.05230	0.03	0.04
5	314.42	−119.1	5.47	1.95477	0.03	0.03
6	314.41	−119.2	5.47	1.88231	0.03	0.04
7	324.78	−109.9	4.78	1.72071	0.01	0.01
8	324.79	−111.2	5.43	1.72815	0.02	0.02
9	335.18	−101.5	4.39	1.71467	0.02	0.02
10	335.16	−100.1	3.77	1.59518	0.03	0.03
11	345.58	−95.0	4.22	1.62894	0.01	0.01
12	345.52	−95.5	4.43	1.63968	0.01	0.01
13	364.36	−82.7	3.54	2.01752	−0.03	0.03
14	364.36	−81.3	2.94	1.73236	−0.04	0.04

(283 to 364) K and in the pressure range from (170 to 5200) kPa. The results are reported in Table 3. The experimental *PVT* measurements were used to derive the second virial coefficient, *B*, and the third virial coefficient, *C*, as described elsewhere.[3,17−18]

In the regression, each run was treated separately, and $(dP)^2$ was used as an objective function, applying the Burnett constant from the helium calibration. The pressure distortion of the Burnett cells was taken into account, as explained elsewhere.[17−18]

Defining the average absolute deviation in pressure as

$$\mathrm{AAD} = \sum_{i=1}^{n} \frac{\mathrm{abs(dP)}}{n} \tag{4}$$

AAD = 0.190 kPa for N_2O was found to be within the estimated experimental uncertainty. The derived second and third virial coefficients for N_2O are given in Table 4, together with the pressure deviations from the fit that always proved to be less than 0.1%. In Figures 3 and 4,

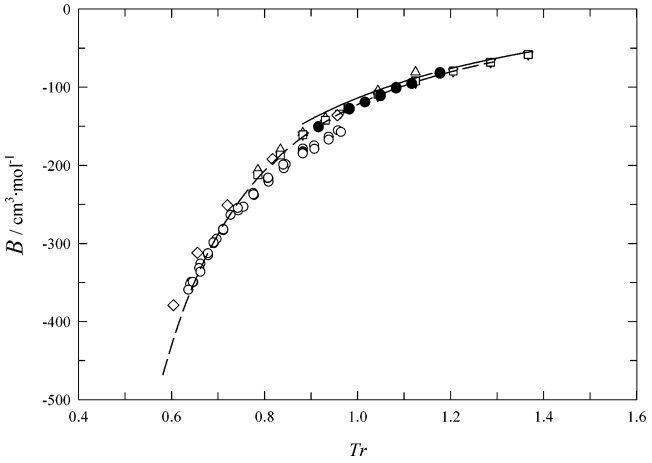

Figure 3. Experimental second virial coefficients for N_2O against reduced temperature, T/T_c, where T_c is the critical temperature: ○, Johnston and Weimer; ▽, Schamp et al.; ●, present work; —, Ihmels and Gmehling; △, Turlington and McKetta; □, Couch et al.; ◇, Elias et al.; – –, Dymond et al.

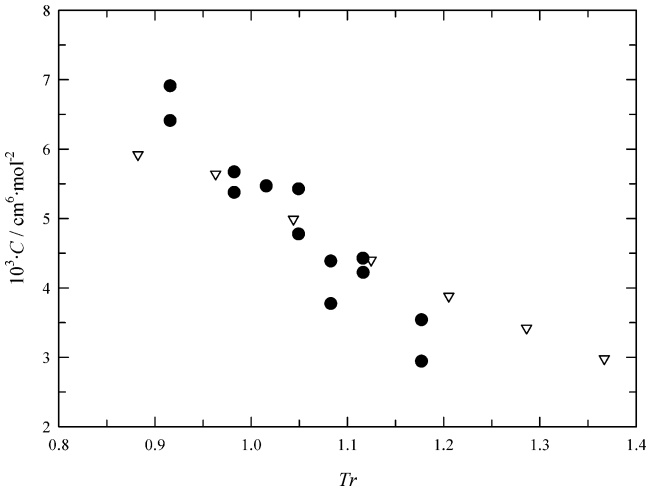

Figure 4. Experimental third virial coefficients for N_2O against reduced temperature: ▽, Schamp et al.; ●, present work.

the second and the third virial coefficients for N_2O are plotted and compared with values in the literature[19−23] and with the calculated recommended equation.[24]

Good agreement between the present data and most of the literature data measured in the reduced temperature range of interest ($0.9 < T_r < 1.2$) is evident both for the second and the third virial coefficients.

Conclusions

In this work, the *PVT* properties of dinitrogen monoxide have been measured both in the saturation region and in the superheated vapor region. The results in the two-phase region were correlated, together with a selection of literature sources, with the Wagner equation. The *PVT* data were also used to derive the second and the third virial coefficients. Good agreement with literature sources was found for all experimental data.

Acknowledgment

We are grateful to Dr. Eric Lemmon for his kind help.

Literature Cited

(1) ASHRAE Standard 34-2001. Designation and Safety Classification of Refrigerant. ASHRAE: Atlanta, GA, 2001.
(2) Di Nicola, G.; Giuliani, G.; Polonara, F.; Stryjek, R. *PVTx* Measurements for the R116 + CO_2 and R41 + CO_2 Systems. New Isochoric Apparatus.*J. Chem. Eng. Data*, submitted for publication, 2004.
(3) Di Nicola, G.; Giuliani, G.; Polonara, F.; Stryjek, R. *PVTx* Measurements for the R125+CO_2 System by the Burnett Methodol. *Fluid Phase Equilib.* **2002**, *199*, 161−174.
(4) Blue, R. W.; Giacque, W. F. The Heat Capacity and Vapor Pressure of Solid and lIquid Nitrous Oxide. The Entropy from its Band Spectrum. *J. Am. Chem. Soc.* **1935**, *57*, 991−997.
(5) Cook, D. The carbon dioxide-nitrous oxide system in the critical region. *Proc. R. Soc. London, Ser. A* **1953**, *219*, 245−256.
(6) Cook, D. The Vapour Pressure and Orthobaric Density of Nitrous Oxide. *Trans. Faraday Soc.* **1953**, *49*, 716−723.
(7) Couch, E. J.; Kobe, K. A.; Hirth, L. J. Volumetric Behavior of Nitrous Oxide. *J. Chem. Eng. Data* **1961**, *6*, 229−233.
(8) Hirth, L. J. Gas Compressibility of Nitrous Oxide and of Sulfur Dioxide by the Burnett Methodol. Ph.D. Dissertation, University of Texas, Austin, TX, 1958 .
(9) Hoge, H. J. Vapor pressure, latent heat of vaporization, and triple-point temperature of N_2O. *J. Res. Natl. Bur. Stand.* **1945**, *34*, 281−293.
(10) Ohgaki, K.; Umezono, S.; Katayama, T. Pressure-Density-Temperature (p-ρ-T) Relations of CHF_3, N_2O, and C_3H_6 in the Critical Region. *J. Supercrit. Fluids* **1990**, *3*, 78−84.
(11) Hunter, M. A. The Molecular Aggregation of Liquefied Gases. *J. Phys. Chem.* **1906**, *10*, 330−360.
(12) Kuenen, J. P. On the condensation and the critical phenomena of mixtures of ethane and nitrous oxide. *J. Philos. Mag.* **1895**, *40*, 173−194.
(13) Parrish, W. R.; Steward, W. G. Vapor−Liquid Equilibria Data for Helium−Carbon Monoxide and Helium−Nitrous Oxide Systems. *J. Chem. Eng. Data* **1975**, *20*, 412−416.
(14) Zeininger, H. Liquid/vapor equilibria of the binary systems N_2O/N_2, N_2O/O_2 and N_2O/CH_4 at low temperatures and high pressures (in German). *J. Chem. Eng. Techol.* **1972**, *44*, 607−612.
(15) Khodeeva, A.; Sokolova, S. M.; Korbutova, E. S. Fugacity of the solute in binary critical solutions at infinite dilution. *J. Phys. Chem.* **1988**, *62*, 576−577.
(16) Li, A.; Kiran, L. Gas−Liquid Critical Properties of Methylamine + Nitrous Oxide and Methylamine + Ethylene Binary Mixtures. *J. Chem. Eng. Data* **1988**, *33*, 342−344.
(17) Glowka, S. Determination of Volumetric Properties of Ammonia Between 298 and 473 K and Carbon Dioxide Between 304 and 423 K Using the Burnett Methodol. *Pol. J. Chem.* **1990**, *64*, 699−709.
(18) Glowka, S. Volumetric Properties of Ammonia + Argon, + Helium, + Methane, and + Nitrogen Mixtures Between 298 and 423 by the Burnett-Isochoric Methodol. *Fluid Phase Equilib.* **1992**, *78*, 285−296.
(19) Turlington, B. L.; McKetta, J. J. The compressibility of carbon dioxide and nitrous oxide at low pressures. *AIChE J.* **1961**, *7*, 336−337.
(20) Schamp, H. W., Jr.; Mason, E. A.; Su, K. Compressibility and intermolecular forces in gases. Nitrous oxide. *J. Phys. Fluids* **1962**, *5*, 769−775.
(21) Johnston, H. L.; Weimer, H. R. Low-Pressure Data of State of Nitric Oxide and of Nitrous Oxide Between their Boiling Points and Room Temperature. *J. Am. Chem. Soc.* **1934**, *56*, 625−630.
(22) Ihmels, E. C.; Gmehling, J. Densities of sulfur hexafluoride and dinitrogen monoxide over a wide temperature and pressure range in the sub- and supercritical states. *Int. J. Thermophys.* **2002**, *23*, 709−743.
(23) Elias, E.; Hoang, N.; Sommer, J.; Schramm, B. The Second Virial Coefficients of Helium Gas Mixtures in the Range Below Room Temperature. *Ber. Bunsen-Ges. Phys. Chem.* **1986**, *90*, 342−351 (German).
(24) Dymond, J. H.; Marsh, K. N.; Wilhoit, R. C.; Wong, K. C. *The Virial Coefficients of Pure Gases and Mixtures*; Springer-Verlag: Berlin, 2002.

Received for review April 23, 2004. Accepted June 21, 2004. This work was supported by MIUR, Ministry of Instruction, University and Research and by the government of the Marche region.

JE049842U